Optimized Inverter Circuits for Driving Dual AC Loads for Home Solar Water Pumping

Devineni Gireesh Kumar[1], *Nagineni* Venkata Sireesha[2], *D S Naga* Malleswara Rao[3] and *Pandla* Chinna Dastagiri Goud[1], *Musheer* Vaqur[4], *T V V* Pavan kumar[5]

[1]Department of EEE, BV Raju Institute of Technology, Narsapur, 502313, Telangana, India
[2]Department of IT, Institute of Aeronautical Engineering, Dundigal, 500043, Telangana, India
[3]Department of EEE, Gokaraju Rangaraju Institute of Engineering & Technology, Bachupally, 500090, Telangana, India
[4]Uttaranchal Institute of Technology, Uttaranchal University, Dehradun, 248007, India
[5]Department of EEE, KG Reddy College of Engineering & Technology, Telangana, 501504, India

Abstract. This research presents a generic pulse width modulation (PWM) approach for nine switch inverters and five-leg inverters. The circuit design of both inverters and a modulation mechanism for separate drives have been described. The available DC bus voltage supplied the two induction motors using a PWM technique for a 5-leg inverter. Nine-switch inverters and nine-switch z-source inverters have lately been presented as dual-output inverter. A nine-switch z-source inverter and a unique pulse width modulation (PWM) were created. Also, a five-leg inverter is modelled using Extended Two Arm Modulation (ETAM) scheme. The suggested modulation techniques were applied to control two machine drive systems with a single inverter architecture with a reduced switch count for pumping the water to house hold appliances. The comparative analysis of the two dual-output inverters is integral to this work.

Keywords. Doubly load system, pulse width modulation, nine switch inverter, and 5-leg inverter, Solar water pumping

1 Introduction

In power electronics, a wide range of converters are employed for various applications. Among them, inverters are crucial in converting DC (Direct Current) power into AC (Alternating Current) power and serving as power controllers for AC motor drives. In certain applications, there is a practical need to control two or more loads simultaneously [1] independently. However, the conventional approach of using individual converters for each load introduces complexities in designing, operating, and maintaining individual converters and their control circuits [2-3]. This paper addresses the challenges associated with controlling two independent loads with a single converter topology while leveraging the power of machine learning techniques. An example of such a system is a washing machine, where separate control of the blower and dryer motor is required during the rinse and spin cycles [4-5]. Employing individual converters for each load raises issues such as increased switch count, elevated switching losses, commutation failures, and complexities in designing control circuits and automation operations [6-8]. Furthermore, industries often employ two-machine drives, necessitating using two independent converters, leading to increased space requirements and separate control circuits [9-11]. To tackle these challenges, this paper proposes a solution by designing a single inverter topology with a reduced switch count and a unified control circuit capable of efficiently driving two loads independently while incorporating machine learning techniques [12-13]. Two design models are presented: the nine-switch inverter and ten-switch inverter, both utilising advanced modulation schemes, namely Sine Pulse Width Modulation (PWM) and Extended Two Arm Modulation (ETAM), respectively [14]. In addition to the advanced modulation techniques, the proposed approach employs machine learning algorithms to optimise the control parameters of the inverters based on real-time operating conditions, load variations, and environmental factors [15]. By learning from historical data and sensor measurements, machine learning models can adaptively adjust the control parameters, improving performance, efficiency, and overall system operation [16]. Machine learning techniques offer several advantages, including enhanced control accuracy, reduced energy losses, and optimised operation [17-19]. By leveraging the power of data-driven algorithms, the control system can make accurate predictions and adaptively optimise control decisions, improving overall system performance [20-22]. This paper elaborates on the design, implementation, and performance evaluation of the proposed nine-switch inverter and ten-switch inverter using Sine Pulse Width Modulation and Extended Two Arm Modulation schemes and integrating machine learning techniques [23-24]. Experimental results and comparisons with the traditional individual converter approach will be presented to demonstrate the effectiveness and benefits of the proposed solution.

2 Proposed Inverter Models

2.1 Structure of Five-Leg Inverter

The Five-Leg Inverter (FLI) is well illustrated in Fig. 1. Five legs make up this inverter. Each leg has related U, V, and W phases for the two motors, with Leg 5 as the common leg for all three phases. E is the direct current (DC)-link voltage.

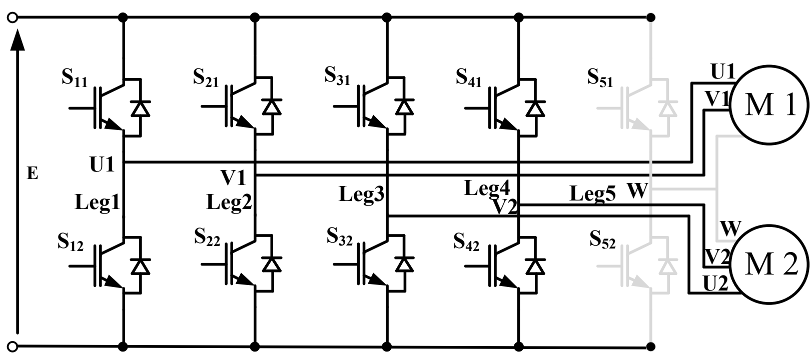

Fig.1. Five-Leg Inverter fed from two Induction Motors

2.2 Structure of nine – switch Inverter

A Nine Level Switch Inverter structure has been shown in Fig.2. It is represented as NSI. This NSI Inverter has three arms connected in series with three switching devices. Motor 1 is connected in the UP phase, and Motor 2 is connected in the down phase. One can notice that one switching state can be reduced compared to the FLI [11].

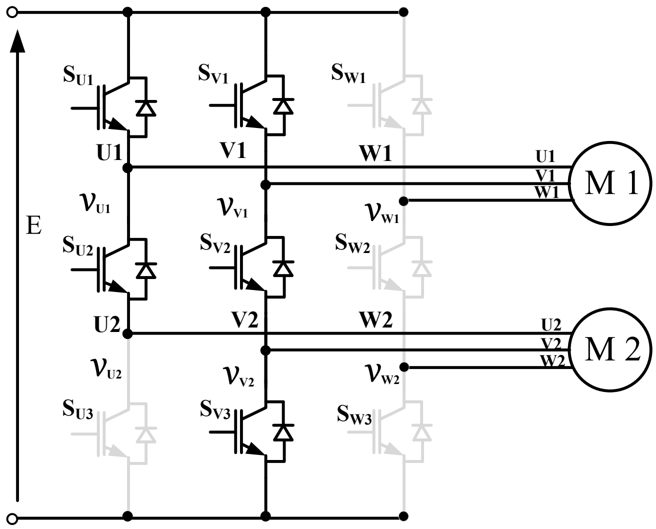

Fig.2. Nine-Switch Inverter fed from two Induction Motors.

3 Modulation Methods of Independent Drives

3.1 An Extended Two-Arm (ETAM) Modulation for Five-Leg Inverter

The extended modulation scheme of 3 leg inverter was developed. i.e. the legs were extended to another two legs. This modulation method is called ETAM (Extended Two Arm Modulation). This method compares carrier waves with zero sequence signals to generate the pulses.

Here a total of two same modules are considered. In this scheme, modular signals are reduced from six to five. A high-frequency carrier is used to compare the reference signals. Below are the signal waves for each phase.

$$\overset{*}{v}_{2arm\_uk} = \overset{*}{v}_{umk} - \overset{*}{v}_{wmk} \text{.......................(1)}$$

$$\overset{*}{v}_{2arm\_vk} = \overset{*}{v}_{vmk} - \overset{*}{v}_{wmk} \text{.......................(2)}$$

$$\overset{*}{v}_{2arm\_wk} = \overset{*}{v}_{wmk} - \overset{*}{v}_{wmk} = 0 \text{...............(3)}$$

v*2arm_ i_k is the gating signal for w plane voltage. The w-phase in both motors is zero when the above gating pulses are given. Hence zero command and gating signals are given. The voltage utility factor is 50%.

Here two motors are facilitated with the five-leg inverter. So it is required to reduce the complexity; also, the control of these motors is done by the DSP. By using this, capital costs can be reduced.

https://doi.org/10.1051/e3sconf/202343001005

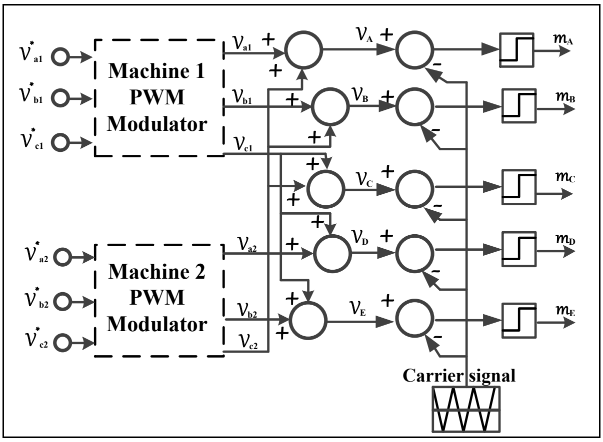

Fig.3. Five-leg VSI using the double zero-sequence injection method for two-motor drive

Harmonics is a major problem in switching. In the previous method, these harmonics will present. This new method can overcome these problems. As it is possible to utilise the zero, line-to-line, and phase-to-phase voltages of the motor, the principle of zero sequence signal injection is a very different manner. The rotating speed of the motors can be shown in Simulink results. From these results, we can clearly say that VUF of the motor 1 is 20(%) and of motor 2 is 80(%).

3.2 Carrier-Based Pulse Modulation Scheme for nine – switch Inverter

A nine-switch inverter's carrier-based PWM scheme is seen in Fig. 4. It had an upper phase and a lower phase in this inverter. Comparing the carrier signal to higher and lower references results in the generation of pulses. It is created individually to provide the upper and lower reference signals. The relationship between V_{refUJ} and the upper phase reference signal is similar. The lower phase reference signal is V_{refLJ} for mid-switch gating signals, which the XOR Logic generates. Continuously two switches will be ON in this method. The carrier-based PWM Vectors are shown in Fig.4 and Fig.5.

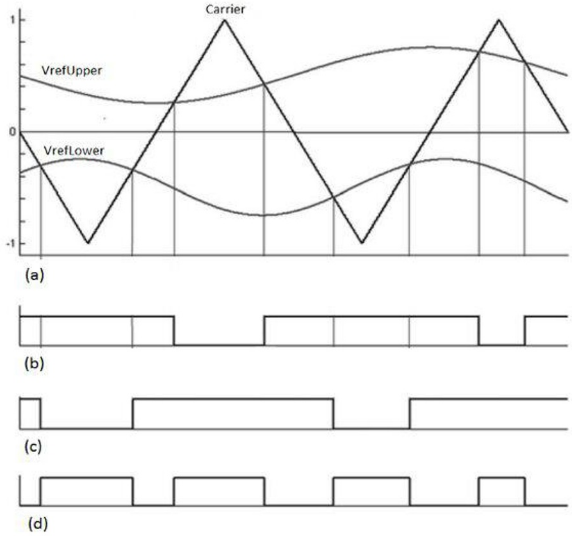

Fig. 4. Nine switch inverter using carrier-based PWM technique.

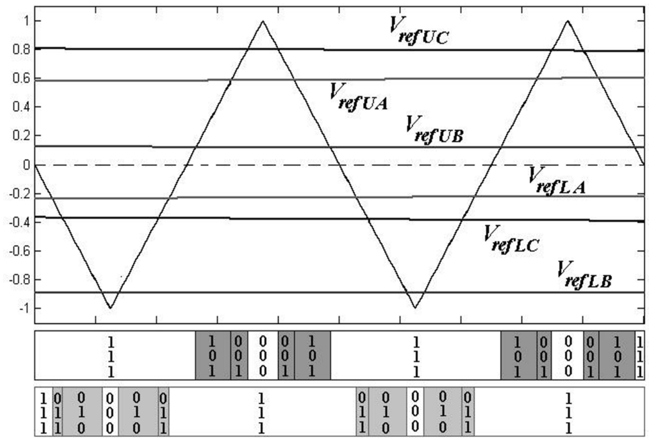

Fig.5. Switching vector for the Carrie-based PWM technique

The formula for a generic modulation rate, m, is

$$m = \frac{v^{ref}}{E/2} \text{..............................(4)}$$

Here, E is a dc supply voltage. The recommended PWM modulation is calculated by adding an offset, E/4, to the reference in (1) and the reference in (2). Therefore,

$$m_{1u} = \frac{v_{u1}^{ref} + E/4}{E/2}. = \frac{v_{1u}^{ref}}{E/2}. + \frac{1}{2} \text{................(5)}$$

$$m_{2u} = \frac{v_{u2}^{ref} - E/4}{E/2}. = \frac{v_{1u}^{ref}}{E/2}. - \frac{1}{2} \text{.................(6)}$$

The reference voltages range from –E/4 and E/4 for *Inv1* and *Inv2*, respectively, from the above equations.

4 Results & Discussions

The five-leg inverter and nine-switch inverters were simulated on MATLAB Simulink Platform with two induction motor loads for both cases, and the results are interpreted as follows.

4.1 for nine-switch inverter_SPWM

The Sine pulse modulation scheme was applied to the nine–switch inverter, and the Line and phase voltages of the nine–switch inverter were plotted as shown below in the figures. Fig.6 represents the Line voltages of *load-1,* and Fig.7 represents the Line voltages of *load-2*. Similarly, Fig.8 represents the Phase voltages of the z-source nine switch inverter for *load -1* (u, v, w phases), and Fig.9 represents the Phase voltages of the z-source nine switch inverter for *load -2* (u, v, w phases).

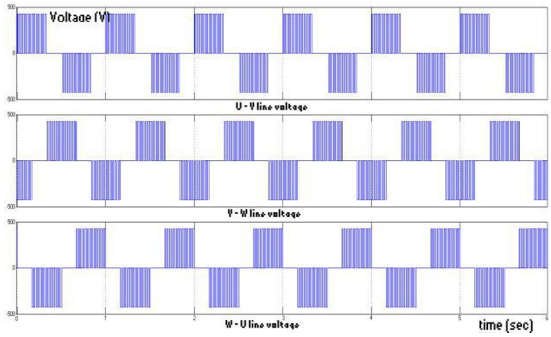

Fig.6. Three-phase line voltages of Load-1

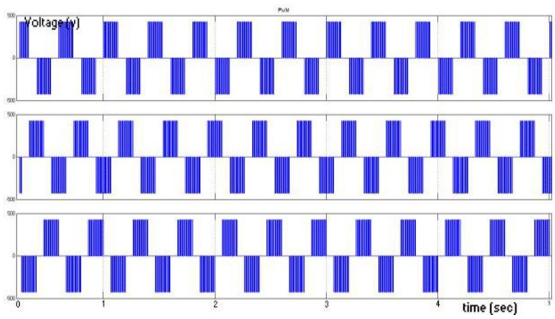

Fig.7. Three-phase line voltages of Load-2

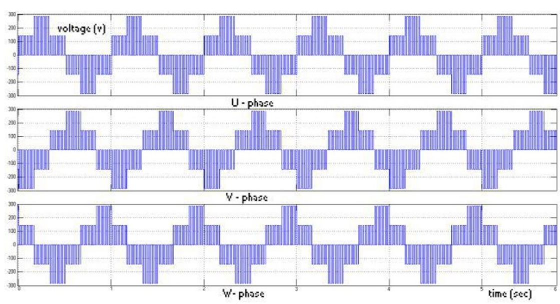

Fig.8. Phase voltages of z-source nine-switch inverter for load -1 (u, v, w phases)

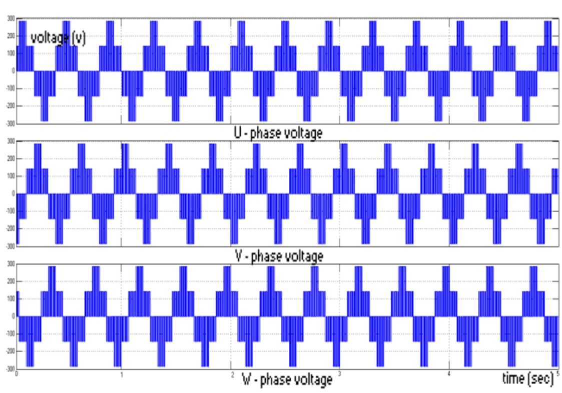

Fig.9. Phase voltages of z-source nine-switch inverter for load -2 (u, v, w phases)

Two identical three-phase induction motors are connected in place of load-1 and load-2 of nine switch inverters, and their characteristics were plotted with a variation of speed considering no load and full load on the induction motors. Fig 10 below shows the Speed-time characteristics of dual motors fed in the inverter output. Fed from nine switch inverters operating with no load, and Fig 11 shows the Speed-time characteristics operating with the load.

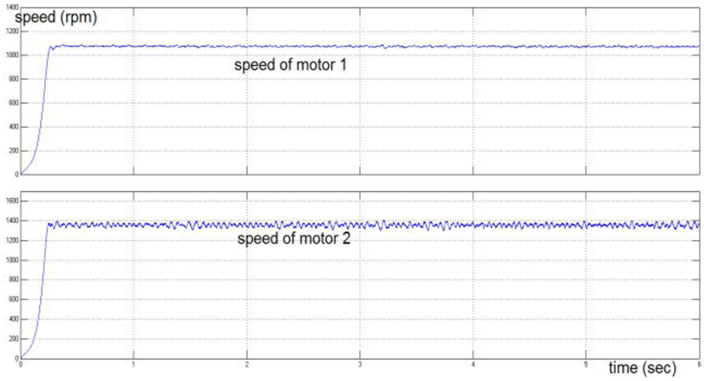

Fig 10. Speed-time characteristics of dual motors fed to the inverter operating with no load.

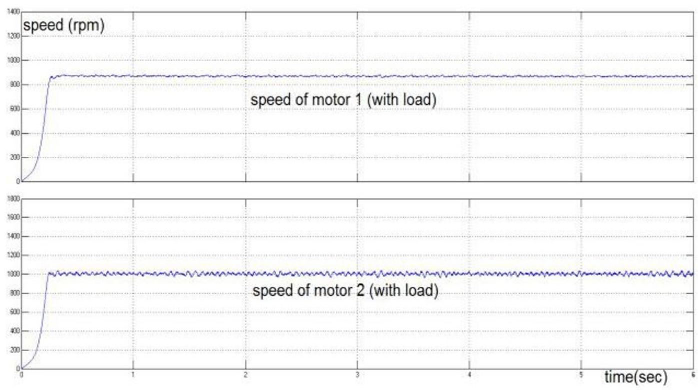

Fig 11. Speed-time characteristics of dual motors fed to the inverter operating with the load.

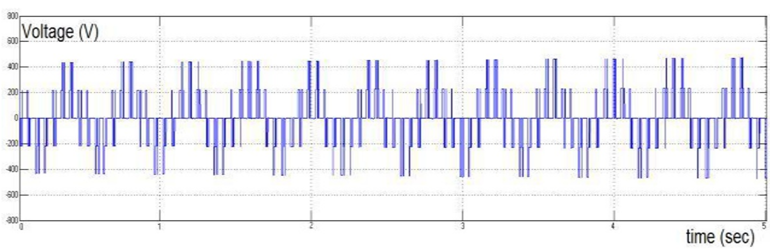

Fig 12. Stator voltage for load-1 (u-phase) of nine-switch inverter

Also, the stator voltages and stator currents of the three-phase induction motor were plotted by considering one of the phases (U-Phase) as shown in Figure 12 for the stator voltage of load -1, figure 13 for the stator voltage of load-2, figure 14 for line currents load-1 and figure 15 for line currents of load-2.

https://doi.org/10.1051/e3sconf/202343001005

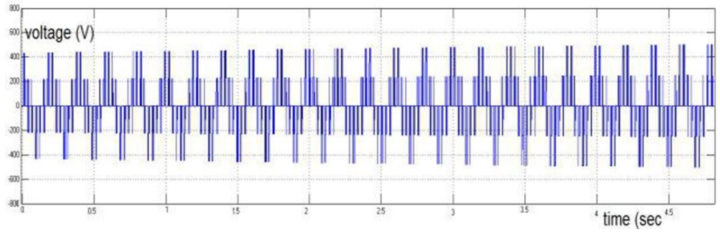

Fig 13. Stator voltage for load-2 (u-phase) of nine-switch inverter

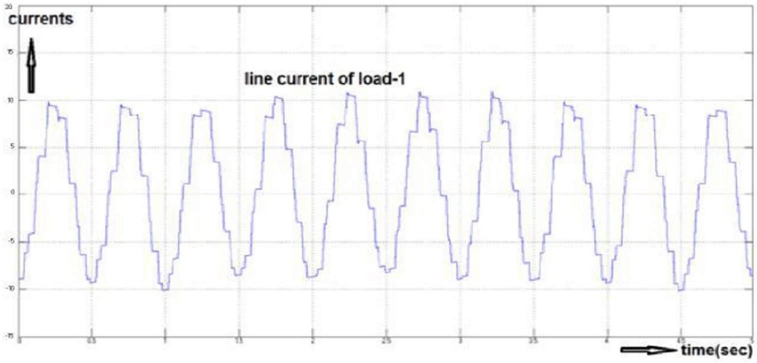

Fig 14. Line currents for load-1 of PWM nine-switch inverter

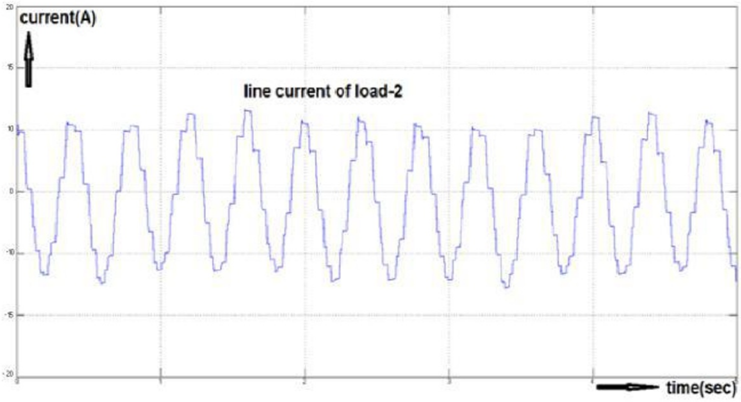

Fig 15. Line currents for load 2 of the PWM nine-switch inverter

4.2 For Five- Leg inverter _ Extended Two Arm Modulation (ETAM)

The Extended Two Arm Modulation (ETAM) was applied to the five-leg inverter, and the performance characteristics of the two loads (Induction motors) were plotted considering no load and full load. Also, the line current characteristics, Loat torque characteristics were plotted as shown in the below figures. Figure 16 depicts the speed-time characteristics of twin motors fed into the inverter output without a load. In contrast, Figure 17 depicts the speed-time characteristics of double motors fed into the inverter output with a load. Figure 18 also depicts the line current characteristics of twin motors feeding into the inverter output of a five-leg inverter. The electromagnetic torque characteristics of twin motors supplied into the inverter output for the 5-leg inverter are depicted in Figure 19.

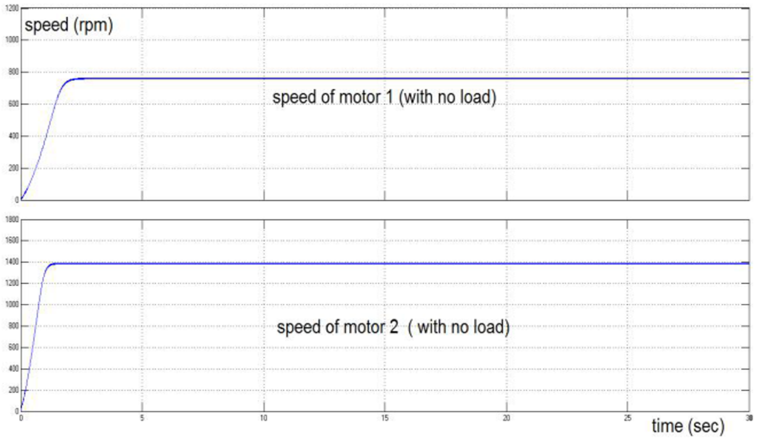

Fig16. Speed-time characteristics of dual motors fed from a 5-leg inverter with no load

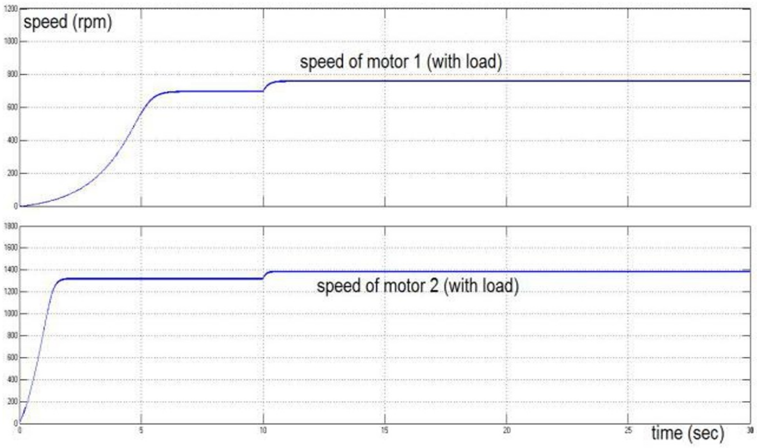

Fig 17. Speed -time characteristics of dual motors fed from a 5-leg inverter with a load

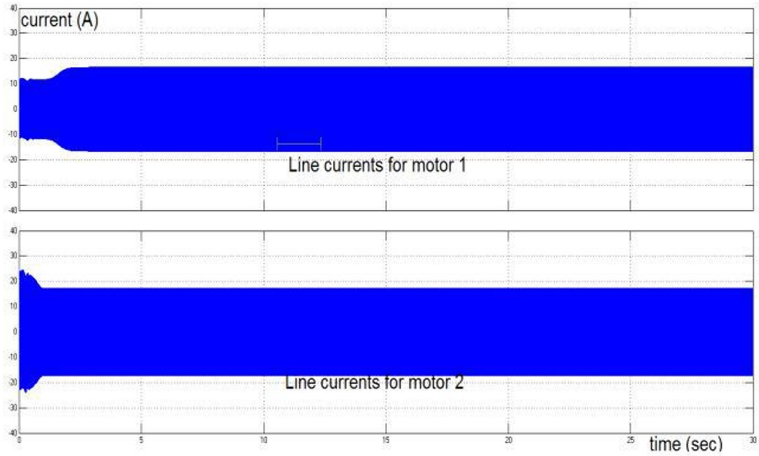

Fig 18. Line current characteristics of dual motors for 5-leg inverter

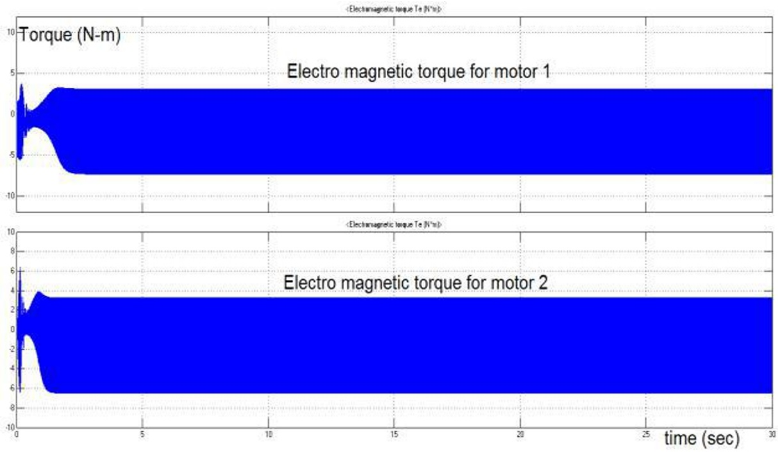

Fig 19. Electromagnetic torque characteristics of dual motors for 5-leg inverter

5 Conclusions

This paper presented two reduced switch inverters for driving two motors independently and simultaneously. The major application of these inverters is in washing machines. To reduce the inverter's size and optimise the control of induction motors, this research proposed a nine-switch and a five-leg dual output inverter. Two three-phase induction motors fed these two inverters. The performance characteristics of two induction motors were analysed using SPWM and ETAM techniques. The speed control results revealed that the five-leg inverter with the ETAM technique gave better operation of the two induction motors than the SPWM with a Nine-switch inverter. However, in cost comparison, the nine-switch inverter is less costly than the five-leg inverter.

References

1. K. Oka, Y. Nozawa, and K. Matsuse, "Improved method of voltage utility factor for PWM control method of the five-leg inverter," 2006 37th IEEE Power Electronics Specialists Conference, Jeju, Korea (South), pp. 1-5, doi: 10.1109/pesc.2006.1711820. (2006).
2. Yang Mei, Lipeng Wang, Zhengxi Li, and K. Matsuse, "An improved modulation method for five-leg inverter," 2013 International Conference on Electrical Machines and Systems (ICEMS), Busan, Korea (South), pp. 2168-2172, doi: 10.1109/ICEMS.2013.6713200. (2013).
3. Hiroyuki Enokijima, Kazuo Oka & Kouki Matsuse (2011) Independent Position Control of Two Permanent Magnet Synchronous Motor Drives Fed by a Five-Leg Inverter, Journal of International Council on Electrical Engineering, 1:4, 400-404, DOI: 10.5370/JICEE.2011.1.4.400. (2011).
4. S. M. Dehghan, M. Mohamadian, and A. Y. Varjani, "A New Variable-Speed Wind Energy Conversion System Using Permanent-Magnet Synchronous Generator and Z-Source Inverter," in IEEE Transactions on Energy Conversion, vol. 24, no. 3, pp. 714-724, doi: 10.1109/TEC.2009.2016022. (2009).
5. T. Kominami and Y. Fujimoto, "A Novel Nine-Switch Inverter for Independent Control of Two Three-Phase Loads," 2007 IEEE Industry Applications Annual Meeting, New Orleans, LA, USA, pp. 2346-2350, doi: 10.1109/07IAS.2007.354. (2007).

6. E. Ledezma, B. McGrath, A. Munoz, and T. A. Lipo, "Dual AC-drive system with a reduced switch count," in IEEE Transactions on Industry Applications, vol. 37, no. 5, pp. 1325-1333, doi: 10.1109/28.952508. (2001).
7. C. Liu, B. Wu, N. R. Zargari, D. Xu and J. Wang, "A Novel Three-Phase Three-Leg AC/AC Converter Using Nine IGBTs," in IEEE Transactions on Power Electronics, vol. 24, no. 5, pp. 1151-1160, doi: 10.1109/TPEL.2008.2004038. (2009).
8. K. Oka, Y. Nozawa, R. Omata, K. Suzuki, A. Furuya, and K. Matsuse, "Characteristic Comparison between Five-Leg Inverter and Nine-Switch Inverter," 2007 Power Conversion Conference, pp. 279-283, doi 10.1109/PCCON.2007.372981. (2007).
9. S. M. Dehghan Dehnavi, M. Mohamadian, A. Yazdian, and F. Ashrafzadeh, "Space Vectors Modulation for Nine-Switch Converters," in IEEE Transactions on Power Electronics, vol. 25, no. 6, pp. 1488-1496, doi: 10.1109/TPEL.2009.2037001. (2010).
10. Devineni, G.K., Ganesh, A. Problem formulations, solving strategies, implementation methods & applications of selective harmonic elimination for multilevel converters. Journal Européen des Systèmes Automatisés, Vol. 53, No. 6, pp. 939-952. https://doi.org/10.18280/jesa.530620. (2020).
11. D.G Kumar, A. Ganesh, “Technological developments in direct grid-connected power converters for solar PV power plants”, International journal of engineering and advanced technology, Vol. 9, No. 1, pp: 6604-6615, doi:10.35940/eject.A1857.109119. (2019).
12. Z. Yang, J. Sun, X. Zha, and Y. Tang, “Power decoupling control for capacitance reduction in cascaded H-bridge converter-based regenerative motor drive systems,” IEEE Transactions on Power Electronics, doi: 10.1109/ TPEL. 2018. 2818719, (2018)
13. D. G. Kumar, A. Ganesh and D. S. Naga Malleswara Rao, "Design and Analysis of a Novel Cascaded 15-Level Asymmetric Inverter Using PSO and Whale Algorithms," 2021 International Conference on Sustainable Energy and Future Electric Transportation (SEFET), Hyderabad, India, pp. 1-6, doi: 10.1109/SeFet48154.2021.9375752. (2021).
14. Devineni Gireesh Kumar, D S Naga Malleswara Rao, Ranjith Kumar Gatla, Saravanan S “Grid Integration of Photovoltaic System with a Single-Phase Reduced Switch Multilevel Inverter Topology”, 2022 IEEE 2nd International Conference on Sustainable Energy and Future Electric Transportation, 10.1109/SeFeT55524.2022.9909189
15. Gatla, R.K., Kshatri, S.S., Sridhar, P., Malleswararao, D.S., Kumar, D.G., Kumar, A.S., Lu, J.H. (2022). Impact of mission profile on reliability of grid-connected photovoltaic inverter. Journal Européen des Systèmes Automatisés, Vol. 55, No. 1, pp. 119-124. https://doi.org/10.18280/jesa.550112
16. Sainadh Singh Kshatri, D S Naga Malleswara Rao, P. Chandra Babu, Devineni Gireesh Kumar, “Reliability Evaluation of PV Inverter Considering Impact of Reactive Power Injection”, 2022 IEEE 2nd International Conference on Sustainable Energy and Future Electric Transportation, 04-06 August 2022, Hyderabad, 10.1109/SeFeT55524.2022.9909259
17. Kshatri, S.S., Sireesha, N.V., Rao, D.S.N.M., Gatla, R.K., Kumar, T.K., Babu, P.C., Saravanan, S., Bhoopal, N., Kumar, D.G. (2023). Reliability assessment of hybrid silicon-silicon carbide IGBT implemented on an inverter for photo voltaic applications. Journal of New Materials for Electrochemical Systems, Vol. 26, No.1, pp. 1-6. https://doi.org/10.14447/jnmes.v26i1.a01
18. Kumar, D.G., Sireesha, N.V., Rao, D.S.N.M., Kasireddy, I., Narukullapati, B.K., Gatla, R.K., Babu, P.C., Saravanan, S. (2023). Modelling of symmetric switched capacitor multilevel Inverter for high power appliances. Journal of New Materials for Electrochemical Systems, Vol. 26, No. 1, pp. 18-25. https://doi.org/10.14447/jnmes.v26i1.a03
19. Kumar, D.G., Bhoopal, N., Ganesh, A., Sireesha, N.V., Rao, D.S.N.M. (2023). Implementation of an asymmetric multilevel inverter for solar photovoltaic applications

using N-R approach. Journal of New Materials for Electrochemical Systems, Vol. 26, No. 1, pp. 7-17. https://doi.org/10.14447/jnmes.v26i1.a02
20. Kumar, M., Gupta, S., Gao, X.-Z., Singh, A. “Plant Species Recognition Using Morphological Features and Adaptive Boosting Methodology”, (2019) IEEE Access, 7, art. no. 8894140, pp. 163912-163918, 10.1109/ACCESS.2019.2952176
21. Upadhyay, R.K., Iyengar, S.R.K. “Introduction to Mathematical Modelling and Chaotic Dynamics” (2013) Introduction to Mathematical Modelling and Chaotic Dynamics, pp. 1-349. 10.1201/b15317
22. Vasanthaseelan, S., Manoj Kumar, P., Anandkumar, R., Hari Ram, K., Subbiah, R., Suresh, V., Abishek, A.S., Anith, R., Aravinth, P., Balaji, S.V. “Investigation on solar water heater with different types of turbulators”, (2021) Materials Today: Proceedings, 47, pp. 5203-5208, 10.1016/j.matpr.2021.05.530
23. Mohammad, M.N., Kumari, Ch.U., Murthy, A.S.D., Jagan, B.O.L., Saikumar, K. “Implementation of online and offline product selection system using FCNN deep learning: Product analysis”, (2021) Materials Today: Proceedings, 45, pp. 2171-2178. 10.1016/j.matpr.2020.10.072
24. Karthik Rao, R., Bobba, P.B., Suresh Kumar, T., Kosaraju, S. “Feasibility analysis of different conducting and insulation materials used in laminated bus bars”, (2019) Materials Today: Proceedings, 26, pp. 3085-3089. 10.1016/j.matpr.2020.02.638.